Catalysis Letters Vol. 101, Nos. 3–4, June 2005 (© 2005)
DOI: 10.1007/s10562-005-4885-3

Favorable synergetic effects between CuO and the reactive planes of ceria nanorods

Kebin Zhou[a], Run Xu[a], Xiaoming Sun[a], Hongde Chen[b], Qun Tian[b], Dixin Shen[b], and Yadong Li[a,*]

[a]*Department of Chemistry, Tsinghua University, Beijing, P.R. China*
[b]*Research Center for Eco-Environmental Sciences, Chinese Academy of Sciences, Beijing, P.R. China*

Received 12 September 2004; accepted 1 February 2005

High-energy, more reactive {001} and {110} planes of CeO_2 nanorods were found to generate favorable synergetic effects between CuO and ceria, resulting in significant enhancement of the copper catalyst performance for CO oxidation.

KEY WORDS: synergetic effect; CuO; CeO_2 nanorods; CO oxidation.

1. Introduction

In recent years, CuO/CeO_2 catalysts have attracted much attention owing to their unique catalytic performances, especially for the complete oxidation of CO [1–3]. Their activities are even comparable to precious metals and it is well accepted that the high activity of CuO/CeO_2 was attributed to the quick reversible Cu^{2+}/Cu^{+} redox couples of highly dispersed copper species [4, 5]. Meanwhile, the redox properties of ceria were generally regarded to play key roles in governing the catalytic behaviors by assisting the $Cu^{2+}/Cu^{+}(Cu^{0})$ couples through Ce^{4+}/Ce^{3+} cycles [4,5]. This suggests that the nature of ceria is needed to be taken into account for designing high performance catalysts. Since nanometer sized particles usually exhibit unique physical and chemical properties, significant progress has been made in controlling the size of ceria nanoparticles [6–8].

On the other hand, it is well known that the reactivity for structure sensitive reaction depends on the crystal plane of the catalyst [9,10]. There are three low-index planes in the ceria fluorite cubic structure, namely the very stable and neutral {111} plane, the less stable {110} plane, and the higher-energy {001} plane [11]. Previous computer simulations predicted that the energy required to create oxygen vacancies on the planes was related to their stabilities. The stability of the {111} plane is greater than that of {001} or {110}, thus it is inherently less reactive as compared with others [12]. Thus controlling the shape of nanocrystals is an equally important aspect of desired catalysts synthesis. However, the "classically" prepared ceria nanoparticles usually exposed the most stable {111} planes, resulting in lower reactivity (the structural models of these nanoparticles are drawn in Figure 1(a)) [11, 13–15].

* To whom correspondence should be addressed.
E-mail: ydli@tsinghua.edu.cn

Recently, through a facile solution-based hydrothermal method we had synthesized one-dimensional CeO_2 nanorods and found that they predominantly exposed more reactive {001} and {110} planes (the structural model of ceria nanorods is drawn in figure 1(b)) and exhibited stable facile redox properties [15]. This implies the CeO_2 nanorods may perform better than the "classical" nanoparticles in assisting the $Cu^{2+}/Cu^{+}(Cu^{0})$ couples [16]. Herein, we report a comparative study of CeO_2 nanorods and nanoparticles as supports for CuO catalysts. A significant enhancement of the copper catalyst activity for CO oxidation has been achieved over CuO/CeO_2-nanorods.

2. Experimental

2.1. Catalysts preparation

The CeO_2 nanoparticles and nanorods were synthesized by the traditional precipitation method and hydrothermal method, respectively [15]. The ceria-supported CuO catalysts were prepared by a deposition–precipitation method as follows. The obtained ceria were suspended in water. To this suspension, an aqueous solution of $Cu(NO_3)_2$ (0.1 M) was added while stirring. During this process, the suspension was kept constant at a pH of about 9.0 by adding 0.25 M NaOH solution. After an additional 60 min of continuous stirring, the precipitate was filtered and washed. The filtrate was then dried overnight at 80 °C in air and calcined at 400 °C for 4 h. The loading of CuO is 1 wt.% for both of the catalysts.

2.2. Catalytic activity evaluation

The catalytic activities for CO oxidation were evaluated in a fixed-bed quartz tubular reactor. 0.4 g of catalyst particles was placed in the reactor. The reactant

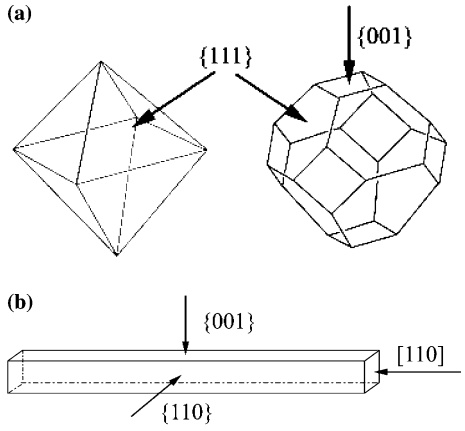

Figure 1. Structural models of ceria nanocrystals. (a) the "classical" prepared ceria nanoparticles, (b) ceria nanorods.

gases (1.0% CO, 2% O_2, 97% N_2) went through the reactor with a space velocity of 120,000 h^{-1}, while the temperature was increased continuously to 200 °C at a rate of 2°C min^{-1}. The composition of the gas exiting the reactor was monitored by gas chromatography.

2.3. Catalyst characterization

Powder XRD was performed on a Bruker D8 Advance X-ray diffractometer with monochromatized $Cu_{K\alpha}$ radiation (λ = 1.5418 Å). The size and morphology of all the materials were measured by using a Hitachi H-800 transmission electron microscope and a JEOL JEM-2010F high-resolution transmission electron microscope. BET-surface area of catalysts was measured by N_2 adsorption using the single point method. Raman spectra were recorded by using a RM 2000 microscopic confocal Raman spectrometer employing a 633 nm laser beam and a charge coupled detector (CCD) with 1 cm^{-1} resolution. The spectra were recorded by using a 20× objective. EPR measurements were performed by an ER200-SRC-10/12 spectrometer in the X-band at ca. 9.7 GHz. Hydrogen temperature-programmed reduction (TPR) was conducted using a conventional apparatus equipped with a TCD detector. Before the TPR analysis, the samples were treated with pure oxygen at 450°C for 45 min. A molecular sieve trap was placed before the detector to adsorb the produced water. TPR was performed by heating the sample (50 mg) at 10 °C/min to 500 °C in a 5% H_2-N_2 mixture flowing at 40 ml/min.

3. Results and discussion

3.1. Catalyst characterization

Figure 2 shows the TEM images of the as-prepared catalysts. The morphology of the catalysts is similar to that of the pure ceria materials. The CuO/CeO_2-nanoparticles exhibit irregular shapes (figure 2(a)). On the other hand, ceria nanorods 100–300 nm in length and about 13–20 nm in diameter are observed in the CuO/CeO_2-nanorods (figure 2(b)). The TEM results indicate the addition of copper has no influence on ceria morphology.

The XRD patterns (figure 3) shows that both the catalysts can be indexed to the pure fluorite cubic structures and no copper species peaks can be observed, indicating high dispersion of copper species on ceria, which was well documented for the CuO/CeO_2 catalysts [1,5,17]. The BET surface area of the CuO/CeO_2 nanorods is

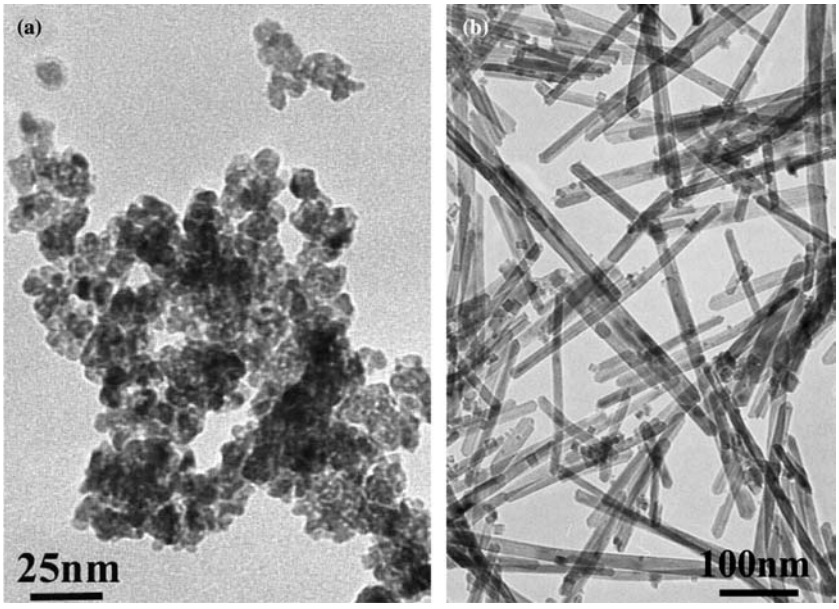

Figure 2. TEM images the catalysts: (a) CuO/CeO_2-nanoparticles and (b) CuO/CeO_2-nanorods.

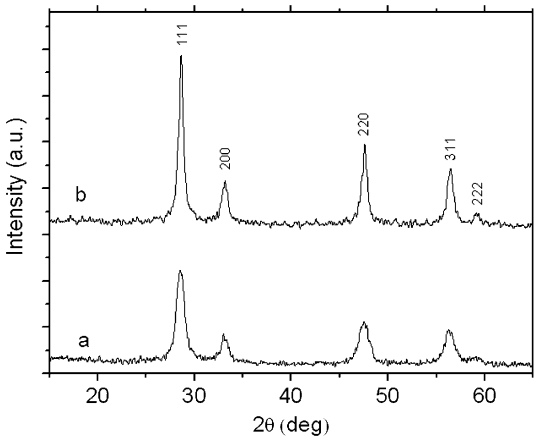

Figure 3. XRD patterns of the catalysts: (a) CuO/CeO_2-nanoparticles and (b) CuO/CeO_2-nanorods.

48 m^2/g, and that of the CuO/CeO_2-nanoparticles is 64 m^2/g. The mean size of ceria nanoparticles in the CuO/CeO_2-nanoparticles is about 8 nm calculated form Scherrer's equation.

Raman spectra of pure CeO_2 and CuO/CeO_2 samples are shown in figure 4. The spectra of CeO_2 nanoparticles (figure 4 (a)) and nanorods (figure 4 (b)) show a strong Raman band at about 462 cm^{-1}, which have been attributed to the contribution of the CeO_2 surface due to the F_{2g} Raman active mode characteristic of fluorite structure materials [18–20]. However, the peak intensities are decreased for the CuO/CeO_2-nanoparticles (figure 4 (c)) and CuO/CeO_2 nanorods (figure 4 (d)), compared with the pure ceria samples, respectively. It is well known that the decreased Raman intensity of ceria in the CuO/CeO_2 samples is strongly related to the coverage of the CeO_2 surface by the dispersed copper oxide species [20]. And this is consistent with the XRD results.

The nature of the copper oxide components of the catalysts has been characterized by EPR spectroscopy (not show). It was found that both of the catalysts comprise isolated Cu^{2+} ions and amorphous CuO clusters, and no larger microcrystals have been observed.

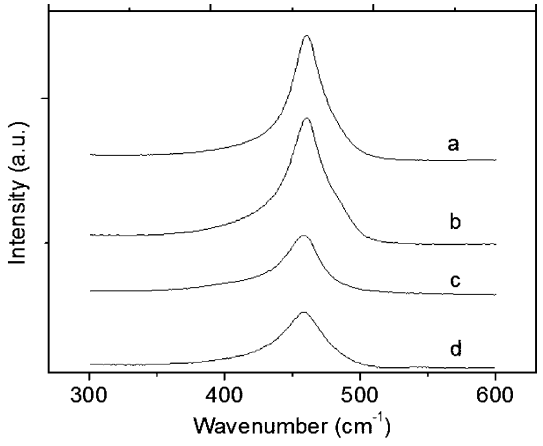

Figure 4. Raman spectra of the samples. (a) CeO_2 nanoparticles, (b) CeO_2 nanorods, (c) CuO/CeO_2-nanoparticles and (d) CuO/CeO_2-nanorods.

The HRTEM images of the catalysts are shown in figure 5. Both of the catalysts generally exhibit ceria crystallites with some highly dispersed amorphous species, but no traces of crystalline copper oxides. The most frequently observed crystal lattice planes of CeO_2 are d_{111} (0.31 nm) in the CuO/CeO_2 nanoparticles, while d_{220} (0.19 nm) is observed in the case of CuO/CeO_2 nanorods. These are consistent with our previous studies [15].

H_2-TPR experiments were performed on the catalysts to reveal their redox properties (figure 6). For both samples, two reduction peaks are observed below 450 °C. The amounts of consumed hydrogen are calculated and excess hydrogen uptake than what is needed to reduce Cu^{2+} to Cu^0 are found, implying that some Ce^{4+} ions get reduced at lower temperature than the pure ceria and pure CuO [21–22]. According to Bera *et al.* [22], the first peak can be assigned to the reduction of -Cu^{2+}-O-Cu^{2+}- dimer of highly dispersed copper oxide and the second peak to the -Cu^{2+}-O-Ce^{4+}- type of species present in the catalyst materials. The first peaks center at 196 and 226°C for the CuO/CeO_2-nanorods and CuO/CeO_2-nanoparticles, respectively. The lower reduction temperature of the CuO/CeO_2-nanorods means the higher reducibility of the highly dispersed copper oxide in this catalyst. The second peaks center at 240 and 263°C for the CuO/CeO_2-nanorods and CuO/CeO_2-nanoparticles, respectively. This provides further evidence of the higher reducibility of the CuO/CeO_2-nanorods. Moreover, the intensity of the second peak of CuO/CeO_2-nanorods is stronger than the CuO/CeO_2-nanoparticles, indicating facile $Cu^{2+}/Cu^{+}(Cu^0)$ couples and Ce^{4+}/Ce^{3+} cycles. The above results reveal a synergetic effect between copper oxide and ceria in these catalysts; especially CeO_2 nanorods perform better than the nanoparticles to assist the $Cu^{2+}/Cu^{+}(Cu^0)$ couples, indicating more favorable synergetic effects between CuO and ceria nanorods compared to the nanoparticles.

3.2. Activity studies

The catalytic activity studies for CO oxidation were carried out and the results are shown in figure 7. It is clear that the CuO/CeO_2-nanorods are more active than the CuO/CeO_2-nanoparticles, although the BET surface area of the former is lower than the latter. Significantly, catalytic activity is found at temperatures as low as 50 °C over CuO/CeO_2-nanorods. The temperature of 100 % conversion of CO to CO_2 is 150 °C over the CuO/CeO_2-nanorods. For the CuO/CeO_2-nanoparticles, the conversion value is 97 % at 200 °C.

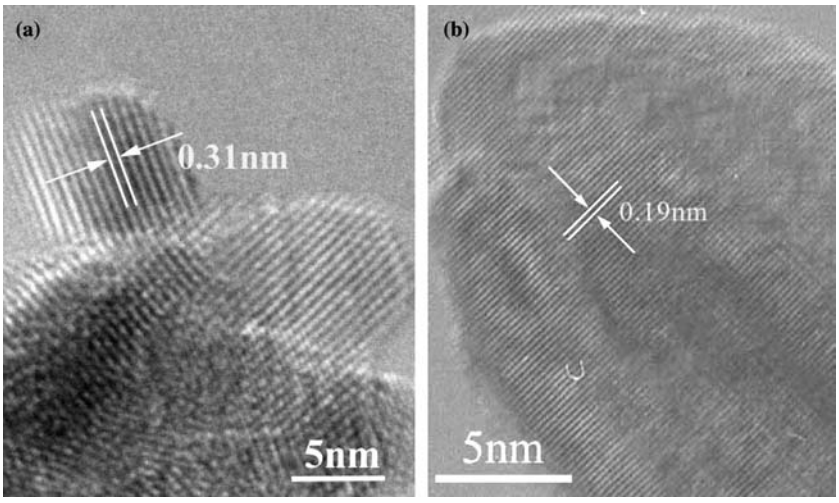

Figure 5. HRTEM imagines of the catalysts (a) CuO/CeO_2-nanoparticles and (b) CuO/CeO_2-nanorods.

Thus, one central question evolves: Why do the CuO/CeO_2 nanorods with lower surface area and larger diameter perform better than the CuO/CeO_2 nanoparticles with higher surface area and smaller particle size? According to our previous study [15], the ceria nanoparticles predominantly exposed the most stable {111} planes, while high-energy, more reactive {001} and {110} planes were predominantly exposed on CeO_2 nanorods. And the nanorods exhibit more stable facile redox properties than the nanoparticles. Through the rf magnetron sputtering method, Skårman *et al.* [16] had successfully prepared two types of ceria films, one with exclusively of {111} type planes and the other with {001} planes. And they reported that the activity of copper oxide supported on {001} planes of CeO_2 film is higher than on {111} planes. Our present activity evaluation results show that the CuO/CeO_2-nanorods are more active than the CuO/CeO_2-nanoparticles. These activity trends are in good agreement with the results obtained by Skårman et al [16]. Moreover, the TPR analysis reveals more favorable synergetic effect between CuO and ceria nanorods compared to the nanoparticles. Therefore, the significant enhancement of catalytic activity over CuO/CeO_2-nanorods is due to the high-energy, reactive ceria planes, which can generate strong synergetic effects between CuO and ceria to assist the copper oxide in changing valence ($Cu^{2+}/Cu^{+}(Cu^0)$) and the ceria in supplying oxygen (Ce^{4+}/Ce^{3+}) for the CO oxidation process.

4. Conclusions

CuO/CeO_2-nanorods were more active for CO oxidation than the CuO/CeO_2-nanoparticles. TPR studies revealed a more favorable synergetic effect between CuO and ceria over CuO/CeO_2-nanorods compared to CuO/CeO_2-nanoparticles. HRTEM results indicated the more favorable synergetic effect over CuO/CeO_2-nanorods could be ascribed to the predominantly exposed high-energy, more reactive crystal planes of ceria nanorods. The present results indicate that high performance of CuO catalysts can be obtained by carefully

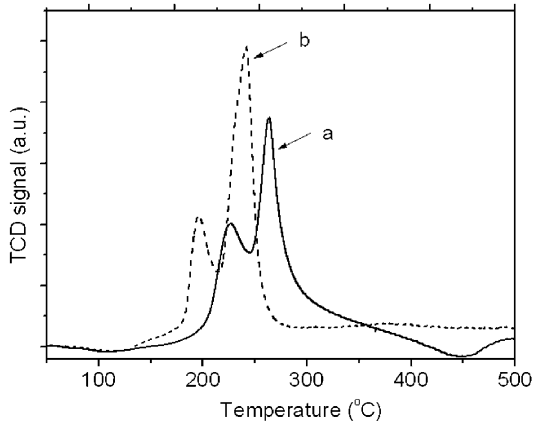

Figure 6. H_2-TPR profiles of the catalysts: (a) CuO/CeO_2-nanoparticles and (b) CuO/CeO_2-nanorods.

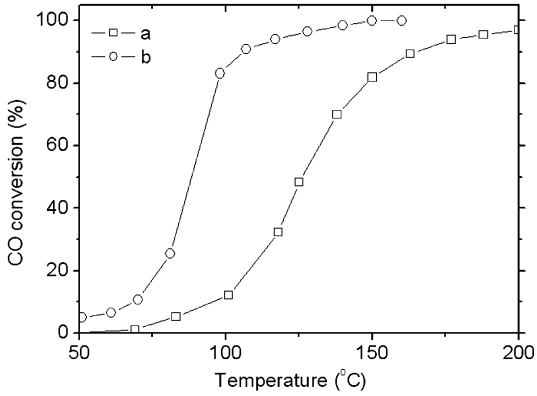

Figure 7. CO conversion vs. reaction temperature over the catalysts: (a) CuO/CeO_2-nanoparticles and (b) CuO/CeO_2-nanorods.

controlling the exposed planes of ceria and this rule may also be adapted to many other supported catalysts.

Acknowledgment

This work was supported by NSFC (90406003, 20401010, 50372030,20025102, 20131030), the Foundation for the Author of National Excellent Doctoral Dissertation of P. R. China and the state key project of fundamental research for nanomaterials and nanostructures (2003CB716901).

References

[1] W. Liu and M.F. Stephanopoulos, J. Catal. 153 (1995) 304.
[2] P.G. Harrison, I.K. Ball, W. Azelee, W. Daniell and D. Goldfarb, Chem. Mater. 12 (2000) 3715.
[3] A. Martínez-Arias, M. Fernández-García, J. Soria and C. Conesa J., J. Catal. 182 (1999) 367.
[4] X. Tang, B. Zhang, Y. Li, Y. Xu, Q. Xin, and W. Shen, Catal. Today, 93–95 (2004) 191..
[5] B. Skårman, T. Nakayama, D. Grandjean, R.E. Benfield, E. Olsson, K. Niihara and L.R. Wallenberg, Chem. Mater. 14 (2002) 3686.
[6] D. Terribile, A. Trovarelli, C. Leitenburg and G. Dolcetti, Chem. Mater. 9 (1997) 2676.
[7] Q. Fu, A. Weber and M.F. Stephanopoulos, Catal. Lett. 77 (2001) 87.
[8] J.A. Wang, J. Dominguez, A. Montoya, S. Castillo, J. Navarrete, M. Moran-Pineda, J. Reyes-Gasga and X. Bokhimi, Chem. Mater. 14 (2002) 4676.
[9] G.A. Somorjai, The surface science of heterogeneous catalysis, Proceedings of the Robert A. Welch Foundation Conferences on Chemical Research, Houston, Texas, November 9–11, 1981, Heterogeneous Catalysis, vol.XXV, pp. 83–127.
[10] P.L.J. Gunter, J.W. Niemantsverdriet, F.H. Ribeiro and G.A. Somorjai, Catal. Rev. Sci. Eng. 39 (1997) 77.
[11] F. Zhang, Q. Jin and S.-W. Chan, J Appl Phys 95 (2004) 4319.
[12] D.C. Sayle, S.A. Maicaneanu and G.W. Watson, J. Am. Chem. Soc. 124 (2002) 11429.
[13] B. Skårman, D. Grandjean, R.E. Benfield, A. Hinz, A. Andersson and L.R. Wallenberg, J. Catal. 211 (2002) 119.
[14] L. Wang Z. and X. Feng, J. Phys. Chem. B 107 (2003) 13563.
[15] K.B. Zhou, X. Wang, X.M. Sun, Q. Peng and Y.D. Li, J. Catal. 229 (2005) 206.
[16] B. Skårman, L.R. Wallenberg, P.-O. Larsson, A. Andersson, J.-O. Bovin, S.N. Jacobsen and U. Helmersson, J. Catal. 181 (1999) 6.
[17] M.S.P. Francisco, V.R. Mastelaro, P.A.P. Nascente and A.O. Florentino, J. Phys. Chem. B 105 (2001) 10515.
[18] W. Shan, Z. Feng, Z. Li, J. Zhang, W. Shen and C. Li, J. Catal. 228 (2004) 206.
[19] A. Martínez-Arias, A.B. Hungría, M. Fernández-García, J.C. Conesa and G. Munuera, J. Phys. Chem. B 46 (2004) 17983.
[20] L. Dong, Y. Hu, M. Shen, T. Jin, J. Wang, W. Ding and Y. Chen, Chem. Mater. 13 (2001) 4227.
[21] P. Zimmer, A. Tschöpe and R. Birringer, J. Catal. 205 (2002) 339.
[22] P. Bera, K.R. Priolkar, P.R. Sarode, M.S. Hegde, S. Emura, R. Kumashiro and N.P. Lalla, Chem. Mater. 14 (2002) 3591.